

Supporting Information

Controlled Deuterium Labeling of Imidazolium Ionic Liquids to Probe the Fine Structure of the Electrical Double Layer Using Neutron Reflectometry

Kazuhiro Akutsu-Suyama,^{1*} Marina Cagnes,² Kazuhisa Tamura,³ Toshiji Kanaya,⁴ and Tamim A. Darwish^{2**}

¹ Neutron Science and Technology Center, Comprehensive Research Organization for Science and Society (CROSS), 162-1 Shirakata, Tokai-Mura, Naka-gun, Ibaraki 319-1106, Japan.

² Australian Centre for Neutron Scattering and National Deuteration Facility, Australian Nuclear Science and Technology Organisation (ANSTO), Locked Bag 2001, Kirrawee DC, NSW 2232, Australia.

³ Quantum Beam Science Center, Japan Atomic Energy Agency (JAEA), Sayo, Hyogo 679-5148, Japan.

⁴ High Energy Accelerator Research Organization (KEK), 203-1 Shirakata, Tokai-Mura, Naka-gun, Ibaraki 319-1106, Japan.

*E-mail: k_akutsu@cross.or.jp (K. Akutsu)

**E-mail: tamim.darwish@ansto.gov.au (T. A. Darwish)

Table of Contents

Synthesis of deuterated ionic liquids	S2
Anion exchange of deuterated ionic liquid	S7
Stability study of deuterated [C _n mim][Cl]	S7
Neutron reflectivity study	S8
Electrochemical measurement settings for neutron reflectivity measurement	S9
Figures of ESI-MS and NMR data	S10
Neutron reflectivity analysis for the partially deuterated IL	S23
Reference	S23

Synthesis of deuterated ionic liquids

The C_n mim cation molecule was deuterated using a single step deuteration reaction. This reaction was performed using a Parr Reactor (600 mL vessel capacity, 3000 psi maximum pressure, 350°C maximum temperature) (Moline, USA).¹ ^1H -NMR (400 MHz), ^{13}C -NMR (100.6 MHz), and ^2H -NMR (61.4 MHz) spectra were recorded on a Bruker 400 MHz spectrometer at 298 K (Sydney, Australia).¹ Electrospray ionization mass spectra (ESI-MS) (MA, USA) were recorded on a 4000 QTrap AB Sciex spectrometer.¹ Note that since $[C_n\text{mim}][\text{Cl}]$ s are highly hygroscopic, the following synthesis yield, which was treated as an anhydrous ionic liquid, would not be necessarily optimum. All reagents were purchased from Sigma–Aldrich unless otherwise specified.

Synthesis of deuterated $[\text{C}_2\text{mim}][\text{Cl}]$ at 160°C

A mixture of $[\text{C}_2\text{mim}][\text{Cl}]$ (5.32 g), Pt/activated carbon (10% Pt, 0.80 g), and Pd/activated carbon (10% Pd, 0.79 g) in D_2O (120 mL) was loaded into the Parr Reactor. The contents of the reactor were degassed by purging with N_2 gas and then purged with H_2 gas. After sealing the reactor, the mixture was heated to 160°C with constant stirring for 24 h. The reactor was cooled to room temperature, and the contents were filtered through a short plug of Celite to remove the catalyst, which was further washed with H_2O (100 mL). The aqueous filtrate was evaporated to dryness under reduced pressure, and remaining gel like product was dried at 80°C and reduced pressure (20 mbar) for 10 min. The weight of the resulting product was used to calculate the yield of the deuteration reaction. Yield: 5.83 g (102 %, 91.2 %-d). ^1H -NMR (400 MHz, D_2O) δ 1.33 (residual signal), 3.74 (residual signal), 4.08 (residual signal), 7.29 (residual signal), 7.36 (residual signal), 8.58 (residual signal). ^2H -NMR (61.4 MHz, D_2O) δ 1.33 (s), 3.74 (s), 4.07 (s), 7.33 (s), 7.40 (s), 8.61 (s). $^{13}\text{C}\{^1\text{H}\}$ -NMR (101 MHz, D_2O) δ 13.0–13.8 (m), 34.3–35.3 (m), 43.8–44.5 (m), 121.1–121.8 (m), 122.7–123.3 (m), 134.8–135.6 (m). $^{13}\text{C}\{^1\text{H}, ^2\text{H}, d1 = 20 \text{ s}\}$ -NMR (101 MHz, D_2O) δ 13.4 (s), 34.9 (s), 44.0 (s), 121.4 (s), 123.0 (s), 135.2 (s). ESI-MS, ^1H -NMR, and ^2H -NMR data are shown in Fig. S3-1-3.

Synthesis of deuterated $[\text{C}_4\text{mim}][\text{Cl}]$ at 100°C

A mixture of $[\text{C}_4\text{mim}][\text{Cl}]$ (5.02 g), Pt/activated carbon (10% Pt, 0.80 g), and Pd/activated carbon (10% Pd, 0.79 g) in D_2O (120 mL) was loaded into the Parr Reactor. The contents of the reactor were degassed by purging with N_2 gas and then purged with H_2 gas. After sealing the reactor, the mixture was heated to 100°C with constant stirring for 24 h. An aliquot of the reaction mixture was taken out from the reactor, and the contents were filtered through a short plug of Celite to remove the catalyst, which was further washed with H_2O (10 mL). The aqueous filtrate was evaporated to dryness under reduced pressure, and remaining gel like product was dried at 80°C and reduced pressure (20 mbar) for 10 min. The deuteration ratio was estimated by ESI-MS (44.9 %-d). ESI-MS data is shown in Fig. S4.

Synthesis of deuterated $[\text{C}_4\text{mim}][\text{Cl}]$ at 130°C

A mixture of [C₄mim][Cl] (5.02 g), Pt/activated carbon (10% Pt, 0.80 g), and Pd/activated carbon (10% Pd, 0.79 g) in D₂O (120 mL) was loaded into the Parr Reactor. The contents of the reactor were degassed by purging with N₂ gas and then purged with H₂ gas. After sealing the reactor, the mixture was heated to 130°C with constant stirring for 24 h. An aliquot of the reaction mixture was taken out from the reactor, and the contents were filtered through a short plug of Celite to remove the catalyst, which was further washed with H₂O (10 mL). The aqueous filtrate was evaporated to dryness under reduced pressure, and remaining gel like product was dried at 80°C and reduced pressure (20 mbar) for 10 min. The deuteration ratio was estimated by ESI-MS (43.8 %-d). ESI-MS data is shown in Fig. S5.

Synthesis of deuterated [C₄mim][Cl] at 160°C

A mixture of [C₄mim][Cl] (5.24 g), Pt/activated carbon (10% Pt, 0.80 g), and Pd/activated carbon (10% Pd, 0.77 g) in D₂O (120 mL) was loaded into the Parr Reactor. The contents of the reactor were degassed by purging with N₂ gas and then purged with H₂ gas. After sealing the reactor, the mixture was heated to 160°C with constant stirring for 24 h. The reactor was cooled to room temperature, and the contents were filtered through a short plug of Celite to remove the catalyst, which was further washed with H₂O (100 mL). The aqueous filtrate was evaporated to dryness under reduced pressure, and remaining gel like product was dried at 80°C and reduced pressure (20 mbar) for 10 min. The weight of the resulting product was used to calculate the yield of the deuteration reaction. Yield: 5.65 g (99.8 %, 93.3 %-d). ESI-MS data is shown in Fig. S6.

Synthesis of deuterated [C₄mim][Cl] at 180°C

A mixture of [C₄mim][Cl] (5.12 g), Pt/activated carbon (10% Pt, 0.86 g), and Pd/activated carbon (10% Pd, 0.79 g) in D₂O (120 mL) was loaded into the Parr Reactor. The contents of the reactor were degassed by purging with N₂ gas and then purged with H₂ gas. After sealing the reactor, the mixture was heated to 180°C with constant stirring for 24 h. The reactor was cooled to room temperature, and the contents were filtered through a short plug of Celite to remove the catalyst, which was further washed with H₂O (100 mL). The aqueous filtrate was evaporated to dryness under reduced pressure, and remaining gel like product was dried at 80°C and reduced pressure (20 mbar) for 10 min. The weight of the resulting product was used to calculate the yield of the deuteration reaction. Yield: 5.31 g (95.9 %, 94.5 %-d). ¹H-NMR (400 MHz, D₂O) δ 0.77 (residual signal), 1.15 (residual signal), 1.68 (residual signal), 3.75 (residual signal), 4.05 (residual signal), 7.31 (residual signal), 7.36 (residual signal), 8.59 (residual signal). ²H-NMR (61.4 MHz, D₂O) δ 0.74 (s), 1.13 (s), 1.67 (s), 3.74 (m), 4.04 (s), 7.34 (m), 7.39 (s), 8.61 (s). ¹³C{¹H}-NMR (101 MHz, D₂O) δ 11.3–12.2 (m), 17.3–18.2 (m), 29.7–30.6 (m), 34.7–35.6 (m), 48.1–49.2 (m), 121.6–122.2 (m), 122.8–123.6 (m), 135.2–135.9 (m). ¹³C{¹H, ²H, d1 = 20 s}-NMR (101 MHz, D₂O) δ 11.6 (m), 17.5 (s), 30.0 (s), 34.9 (s), 48.5 (s), 121.8 (s), 123.0 (s), 135.5 (s). ESI-MS, ¹H-NMR, and ²H-NMR data are shown in Fig. S7-1-3.

Synthesis of deuterated [C₈mim][Cl] at 160°C

A mixture of [C₈mim][Cl] (4.95 g), Pt/activated carbon (10% Pt, 0.76 g), and Pd/activated

carbon (10% Pd, 0.76 g) in D₂O (120 mL) was loaded into the Parr Reactor. The contents of the reactor were degassed by purging with N₂ gas and then purged with H₂ gas. After sealing the reactor, the mixture was heated to 160°C with constant stirring for 24 h. An aliquot of the reaction mixture was taken out from the reactor, and the contents were filtered through a short plug of Celite to remove the catalyst, which was further washed with H₂O (10 mL). The aqueous filtrate was evaporated to dryness under reduced pressure, and remaining gel like product was dried at 80°C and reduced pressure (20 mbar) for 10 min. The deuteration ratio was estimated by ESI-MS (64.5 %-d). ESI-MS data is shown in Fig. S8.

Synthesis of deuterated [C₈mim][Cl] at 180°C

A mixture of [C₈mim][Cl] (4.90 g), Pt/activated carbon (10% Pt, 0.77 g), and Pd/activated carbon (10% Pd, 0.78 g) in D₂O (120 mL) was loaded into the Parr Reactor. The contents of the reactor were degassed by purging with N₂ gas and then purged with H₂ gas. After sealing the reactor, the mixture was heated to 180°C with constant stirring for 24 h. An aliquot of the reaction mixture was taken out from the reactor, and the contents were filtered through a short plug of Celite to remove the catalyst, which was further washed with H₂O (10 mL). The aqueous filtrate was evaporated to dryness under reduced pressure, and remaining gel like product was dried at 80°C and reduced pressure (20 mbar) for 10 min. The deuteration ratio was estimated by ESI-MS (67.7 %-d). ESI-MS data is shown in Fig. S9.

Synthesis of deuterated [C₈mim][Cl] at 200°C

A mixture of [C₈mim][Cl] (4.90 g), Pt/activated carbon (10% Pt, 0.77 g), and Pd/activated carbon (10% Pd, 0.78 g) in D₂O (120 mL) was loaded into the Parr Reactor. The contents of the reactor were degassed by purging with N₂ gas and then purged with H₂ gas. After sealing the reactor, the mixture was heated to 200°C with constant stirring for 24 h. The reactor was cooled to room temperature, and the contents were filtered through a short plug of Celite to remove the catalyst, which was further washed with H₂O (100 mL). The aqueous filtrate was evaporated to dryness under reduced pressure, and remaining gel like product was dried at 80°C and reduced pressure (20 mbar) for 10 min. The weight of the resulting product was used to calculate the yield of the deuteration reaction. Yield: 4.14 g (78.4 %, 78.0 %-d). ¹H-NMR (400 MHz, D₂O) δ 0.69 (residual signal), 1.10 (residual signal), 1.70 (residual signal), 3.78 (residual signal), 4.07 (residual signal), 7.35 (residual signal), 7.39 (residual signal), 8.70 (residual signal). ²H-NMR (61.4 MHz, D₂O) δ 0.64 (br s), 1.09 (br s), 1.70 (br s), 3.78 (br s), 4.07 (br s), 7.38 (br s), 7.42 (br s), 8.72 (br s). ¹³C{¹H}-NMR (101 MHz, D₂O) δ 12.0–13.6 (m), 20.6–22.2 (m), 24.0–24.9 (m), 26.8–28.8 (m), 29.9–31.2 (m), 34.7–35.8 (m), 48.4–49.3 (m), 121.5–122.2 (m), 122.9–123.6 (m), 135.2–135.9 (m). ¹³C{¹H, ²H, d1 = 20 s}-NMR (101 MHz, D₂O) δ 12.4 (s), 12.7 (s), 13.0 (s), 13.3 (s), 13.6 (s), 20.8 (s), 20.9 (s), 21.0 (s), 21.4 (s), 21.9 (s), 22.0 (s), 22.1 (s), 22.2 (s), 24.3 (s), 24.4 (s), 27.0 (s), 27.2 (s), 27.3 (s), 27.4 (s), 28.2 (s), 28.3 (s), 28.4 (s), 29.9 (s), 31.0 (s), 31.1 (s), 31.2 (s), 34.8 (s), 35.1 (s), 35.3 (s), 48.8 (s), 49.1 (s), 121.8 (s), 123.2 (s), 135.5 (s). ESI-MS, ¹H-NMR, and ²H-NMR data are shown in Fig. S10-1-3. Some small extra signals in the ¹H-NMR data of deuterated [C₈mim][Cl]

were observed which indicates minor impurities. Note that since 1-methylimidazole is soluble in water, we conclude that these signals in the ^1H -NMR data are attributed to the minor impurity of 1-methylimidazole that was generated by the decomposition of C_8mim cation during the hydrothermal reaction.

Synthesis of deuterated $[\text{C}_{10}\text{mim}][\text{Cl}]$ at 160°C

A mixture of $[\text{C}_{10}\text{mim}][\text{Cl}]$ (4.50 g), Pt/activated carbon (10% Pt, 0.79 g), and Pd/activated carbon (10% Pd, 0.78 g) in D_2O (120 mL) was loaded into the Parr Reactor. The contents of the reactor were degassed by purging with N_2 gas and then purged with H_2 gas. After sealing the reactor, the mixture was heated to 160°C with constant stirring for 24 h. An aliquot of the reaction mixture was taken out from the reactor, and the contents were filtered through a short plug of Celite to remove the catalyst, which was further washed with H_2O (10 mL). The aqueous filtrate was evaporated to dryness under reduced pressure, and remaining gel like product was dried at 80°C and reduced pressure (20 mbar) for 10 min. The deuteration ratio was estimated by ESI-MS (49.0 %-d). ESI-MS data is shown in Fig. S11.

Synthesis of deuterated $[\text{C}_{10}\text{mim}][\text{Cl}]$ at 200°C

A mixture of $[\text{C}_{10}\text{mim}][\text{Cl}]$ (4.50 g), Pt/activated carbon (10% Pt, 0.79 g), and Pd/activated carbon (10% Pd, 0.78 g) in D_2O (120 mL) was loaded into the Parr Reactor. The contents of the reactor were degassed by purging with N_2 gas and then purged with H_2 gas. After sealing the reactor, the mixture was heated to 200°C with constant stirring for 24 h. An aliquot of the reaction mixture was taken out from the reactor, and the contents were filtered through a short plug of Celite to remove the catalyst, which was further washed with H_2O (10 mL). The aqueous filtrate was evaporated to dryness under reduced pressure, and remaining gel like product was dried at 80°C and reduced pressure (20 mbar) for 10 min. The deuteration ratio was estimated by ESI-MS (74.7 %-d). ESI-MS data is shown in Fig. S12.

Synthesis of 50 % deuterated $[\text{C}_4\text{mim}][\text{Cl}]$

A mixture of $[\text{C}_4\text{mim}][\text{Cl}]$ (4.83 g), Pt/activated carbon (10% Pt, 0.76 g), and Pd/activated carbon (10% Pd, 0.76 g) in H_2O (60 mL) and D_2O (60 mL) mixture was loaded into the Parr Reactor. The contents of the reactor were degassed by purging with N_2 gas and then purged with H_2 gas. After sealing the reactor, the mixture was heated to 160°C with constant stirring for 24 h. The reactor was cooled to room temperature, and the contents were filtered through a short plug of Celite to remove the catalyst, which was further washed with H_2O (100 mL). The aqueous filtrate was evaporated to dryness under reduced pressure, and remaining gel like product was dried at 80°C and reduced pressure (20 mbar) for 10 min. The weight of the resulting product was used to calculate the yield of the deuteration reaction. Yield: 5.03 g (99.9 %, 48.8 %-d). ^1H -NMR (400 MHz, D_2O) δ 0.79 (m), 1.18 (m), 1.72 (m), 3.76 (m), 4.07 (m), 7.32 (d), 7.36 (d), 8.60 (s). ^2H -NMR (61.4 MHz, D_2O) δ 0.77 (m), 1.16 (br s), 1.67 (br s), 3.78 (m), 4.05 (br s), 7.37 (d), 8.62 (br s). $^{13}\text{C}\{^1\text{H}\}$ -NMR (101 MHz, D_2O) δ 11.5–12.7 (m), 17.6–18.7 (m), 30.2–31.2 (m), 34.8–35.7 (m), 48.6–49.3 (m), 121.9–122.3 (m), 123.2–123.5 (m), 135.6–135.9 (m). $^{13}\text{C}\{^1\text{H}, ^2\text{H}, \text{d1} = 20 \text{ s}\}$ -NMR

(101 MHz, D₂O) δ 12.3 (m), 18.1 (m), 30.7 (t), 35.3 (q), 48.9 (t), 122.0 (t), 123.2 (t), 135.6 (d). ESI-MS and ¹H-NMR data are shown in Fig. S13-1-2.

Synthesis of 70 % deuterated [C₄mim][Cl]

A mixture of [C₄mim][Cl] (5.33 g), Pt/activated carbon (10% Pt, 0.77 g), and Pd/activated carbon (10% Pd, 0.80 g) in H₂O (30 mL) and D₂O (70 mL) mixture was loaded into the Parr Reactor. The contents of the reactor were degassed by purging with N₂ gas and then purged with H₂ gas. After sealing the reactor, the mixture was heated to 160°C with constant stirring for 24 h. The reactor was cooled to room temperature, and the contents were filtered through a short plug of Celite to remove the catalyst, which was further washed with H₂O (100 mL). The aqueous filtrate was evaporated to dryness under reduced pressure, and remaining gel like product was dried at 80°C and reduced pressure (20 mbar) for 10 min. The weight of the resulting product was used to calculate the yield of the deuteration reaction. Yield: 5.61 g (99.3 %, 69.9 %-d). ESI-MS data is shown in Fig. S14.

Synthesis of position-selective deuterated [C₄mim][Cl]

A mixture of [C₄mim][Cl] (5.07 g), Pt/activated carbon (10% Pt, 0.80 g), and Pd/activated carbon (10% Pd, 0.79 g) in H₂O (55 mL) and D₂O (65 mL) mixture was loaded into the Parr Reactor. The contents of the reactor were degassed by purging with N₂ gas and then purged with H₂ gas. After sealing the reactor, the mixture was heated to 160°C with constant stirring for 24 h. The reactor was cooled to room temperature, and the contents were filtered through a short plug of Celite to remove the catalyst, which was further washed with H₂O (100 mL). The aqueous filtrate was evaporated to dryness under reduced pressure, and remaining gel like product was dried at 80°C and reduced pressure (20 mbar) for 10 min. The resulting product (46.6 %-d, equally) was used to the next deuteration reaction.

A mixture of [C₄mim][Cl] (46.6 %-d, 8.60 g), Pt/activated carbon (10% Pt, 0.82 g), and Pd/activated carbon (10% Pd, 0.81 g) in D₂O (120 mL) mixture was loaded into the Parr Reactor. The contents of the reactor were degassed by purging with N₂ gas and then purged with H₂ gas. After sealing the reactor, the mixture was heated to 120°C with constant stirring for 24 h. The reactor was cooled to room temperature, and the contents were filtered through a short plug of Celite to remove the catalyst, which was further washed with H₂O (100 mL). The aqueous filtrate was evaporated to dryness under reduced pressure, and remaining gel like product was dried at 80°C and reduced pressure (20 mbar) for 10 min. The weight of the resulting product was used to calculate the yield of the deuteration reaction. Yield: 5.51 g (63.1 %, 66.1 %-d). ESI-MS, ¹H-NMR, ²H-NMR, ¹³C-NMR data are shown in Fig. S15-1-4.

Starting materials

¹H-NMR data of the starting materials are shown in Fig. S15-1-4.

Anion exchange of deuterated ionic liquid

Anion exchange reaction of [C₄mim][Cl] was conducted according to the method of Z. K. Reeder *et al.*² with minor change.

An aqueous solution of [C₄mim][Cl] (1.98 g, 30 ml) was mixed with an aqueous solution of lithium bis(trifluoromethanesulfonyl)amide (Li-TFSA) (3.59 g, 30 ml). After 1 min shaking, the upper aqueous phase was removed and remaining IL was washed three times with 30 ml of distilled water. The product was purified by silica gel chromatography eluting with ethyl acetate-chloroform to yield 4.06 g (89.7 %) of [C₄mim][TFSA].

Stability Study of deuterated [C_nmim][Cl]

In this study, to reveal the stability of deuterated [C_nmim][Cl], neutron irradiation effect was monitored by fluorescence spectrophotometry. Sample solutions (0.1 mM) were prepared using ethanol-*d*₆ to increase the transmittance of neutron beam, and same sample cells (quartz, total quartz length = 2.0 mm, path length = 1.0 cm) were used in this experiments. The neutron beam size was 10×10 mm² and the total neutron exposure times for the experiments was 1.0 h. After the neutron irradiation, the fluorescence spectra were measured to estimate the concentration of C_nmim cation. Fluorescence measurements were carried out at the fluorescence excitation wavelength of 250 nm. Changes in the fluorescence spectrum can monitor the degradation of C_nmim cation. Note that the samples were not shaken to enhance diffusion of the degraded products. All fluorescence measurements were carried out on a FP-8300 (Nihon Bunko Co., Ltd., Tokyo, Japan) spectrofluorophotometer. Fluorescence spectra are shown in Fig. S1.

Although C_nmim ILs have high chemical and physical stability, the stability of the C₄mim ILs toward neutron beam irradiation was studied by monitoring of the fluorescence intensity of C₄mim cation to make sure that [C₄mim][Cl] did not undergo decomposition during neutron experiment. Sample solutions (0.1 mM) were prepared using ethanol-*d*₆, and quartz cell (path length = 1.0 cm) was used in this experiments. The neutron beam size was fixed to 10×10 mm², and the total neutron exposure times for the experiments was 1.0 h. After the neutron irradiation, the fluorescence spectra were measured to estimate the concentration of C₄mim cation. Figure 1 shows the fluorescence spectra change of [C₄mim][Cl] and [C₄mim-*d*₁₅][Cl] by irradiation of neutron beam. The fluorescence peak of C₄mim cation appears at around 310 nm. As shown in Figure 1, the fluorescence intensity of C₄mim cation did not change by neutron beam irradiation even in deuterated C₄mim cation. Therefore, it can be suggested the concentration of C₄mim cation did not change after neutron beam irradiation, that is, the degradation reaction did not occur during neutron beam irradiation. Previous studies indicated that the mean bond length of C-H bond is clearly greater than that of C-D bond,³ and the C-H bond is thermodynamically more unstable than the corresponding C-D bond.⁴ Thus, we can conclude that the deuteration of C_nmim ILs do not affect

the neutron experiments in terms of stability of C_n mim ILs.

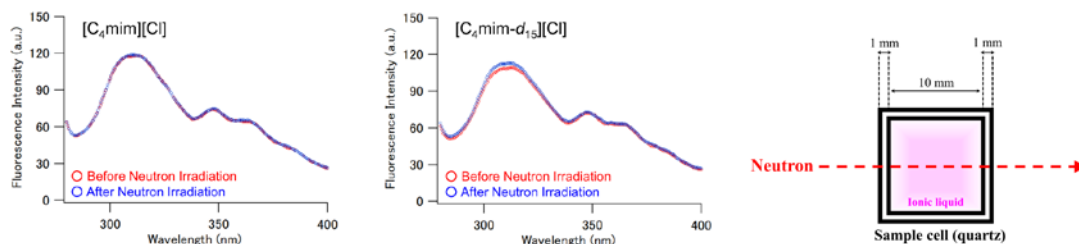


Figure S1 Fluorescence spectra of $[C_4\text{mim}][\text{Cl}]$ and $[C_4\text{mim-}d_{15}][\text{Cl}]$ before and after neutron irradiation, and image of the experimental cell.

Neutron reflectivity measurement

The NR measurements were performed on a BL17 SHARAKU reflectometer installed at the Materials and Life Science Experimental Facility (MLF) in J-PARC.⁵ The incident beam power of the proton accelerator was 150 kW for all the measurements. Pulsed neutron beams were generated using a mercury target at 25 Hz, and the NR data were measured using the time-of-flight (TOF) technique. The neutron-source to sample distance was 15.5 m, and the sample to ^3He gas point detector distance was 2.5 m. The wavelength (λ) range of the incident neutron beam was tuned to be approximately $\lambda = 1.1\text{--}8.8$ Å using disk choppers. The covered Q_z range was $Q_z = 0.01 - 0.24$ Å⁻¹, where $Q_z = (4\pi/\lambda)\sin\theta$ (here, θ represents the incident angle). The incident angle for the samples varied from 0.4° to 1.4°. The total exposure times for the measurements was 9 h. 25 mm beam footprint was maintained on the sample surfaces by using six kinds of incident slits. The samples were placed in a Teflon sample cell on the sample stage, which was installed at the center position of the sample rotator. All the measurements were performed at room temperature.

The data reduction, normalization, and subtraction were performed using a program installed in BL17 SHARAKU that was developed for the TOF data. The Motofit program⁶ was used to fit the NR profiles using the least-squares approach to minimize deviations in the fit; the thickness, scattering length density (SLD), and Gaussian roughness were evaluated by the program. Table S1 shows the structural parameters obtained from this analysis.

Table S1. Best-fit parameters for the reflectivity model data shown in Figure 2.

Layer	Molecule	t (Å)	SLD ($\times 10^{-6}$ Å ⁻²)	σ (Å)
Bulk IL Layer	$[C_4\text{mim}][\text{TFSA}]$	—	5.25	2.26
Diffuse Layer	$[\text{TFSA}]^-$ dominant	11.3	4.92	2.80
	$[C_4\text{mim}]^+$ dominant	11.9	5.51	2.61
Negative Layer	$[\text{TFSA}]^-$	13.5	3.57	2.01
Positive Layer	$[C_4\text{mim}]^+$	7.72	6.53	2.28
Substrate (Negative)	SiO_2	10.5	3.47	2.34
	Si substrate	—	2.07	—

t : thickness (Å), scattering length density (SLD): ρ ($\times 10^{-6}$ Å⁻²), σ : surface or interface roughness (Å).

Electrochemical measurement settings for neutron reflectivity measurement

A cell specially designed for NR measurements was used as an electrochemical cell. It is made of Kel-F. The working electrode was a $40 \times 40 \text{ mm}^2$ square n-Si(100) single-crystal plate with a height of 5 mm (Nihon Exceed Co., Ltd., Japan). Pt wires were used as the reference and counter electrodes. To minimize the solution resistance effect, the reference and counter electrodes were positioned 3 mm above the working electrode.

The deuterated $[\text{C}_4\text{mim}][\text{TFSA}]$ was dehydrated at 80°C under vacuum ($6 \times 10^0 \text{ Pa}$) for 12 h before use. Before measurement, the working electrode was cleaned with ethanol and acetone in an ultrasonic bath. Finally, it was rinsed with Milli-Q water. All the electrodes, $[\text{C}_4\text{mim}][\text{TFSA}]$ and the electrochemical cell were transferred to a glove box filled with Ar gas and they were assembled in the glove box. During NR measurements, the sample cell was set into a N_2 gas (G3 grade) box and the electrode potential was controlled using a potentiostat (IviumStat, Ivium technologies).

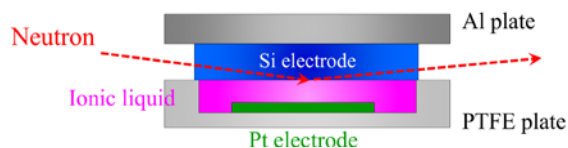


Fig S2. Image of the experimental cell.

Figures of ESI-MS and NMR data

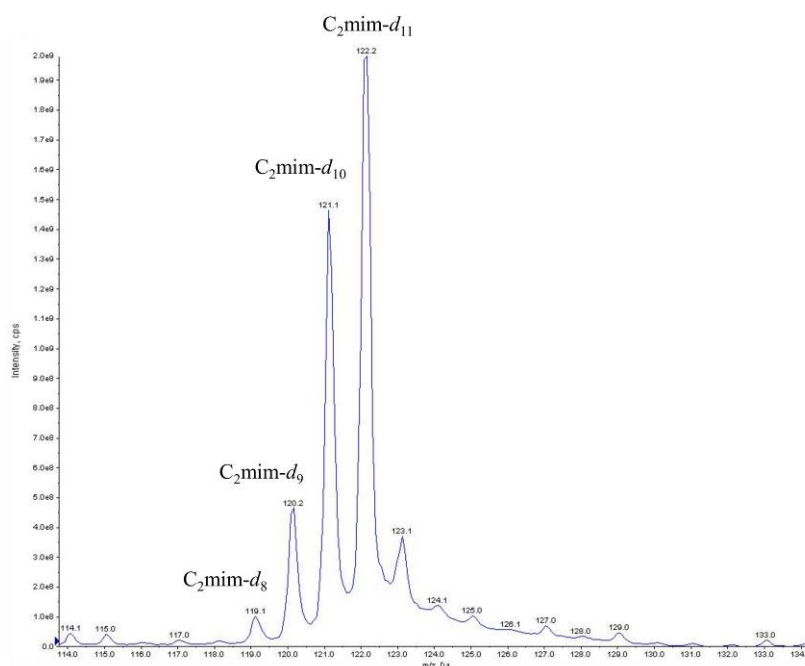


Fig. S3-1. Electrospray ionization mass spectra in positive mode of C_2mim cation showing the mass distribution of the different isotopologues, which ranges from d_8 – d_{11} . The distribution of the isotopologues is as follows (M^+): 4.9 %, d_8 ; 17.8 %, d_9 ; 33.5 %, d_{10} ; 35.0 %, d_{11} .

1H -NMR

$[C_2mim][Cl]$ 91.2%- d

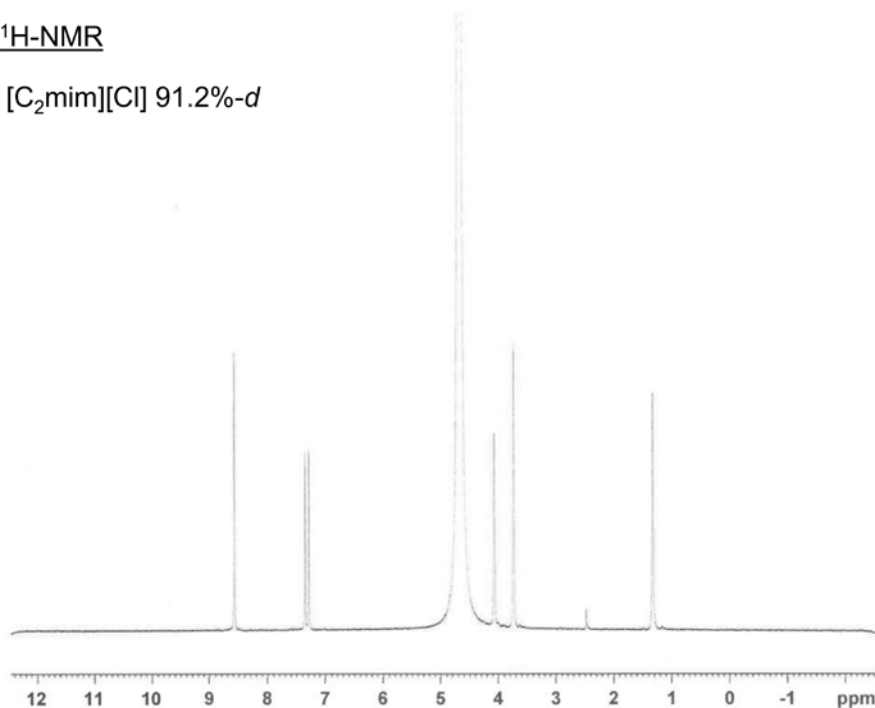


Fig. S3-2. 1H -NMR (D_2O , 400 MHz) of deuterated (91.2%) $[C_2mim][Cl]$.

^2H -NMR

$[\text{C}_2\text{mim}][\text{Cl}]$ 91.2%-*d*

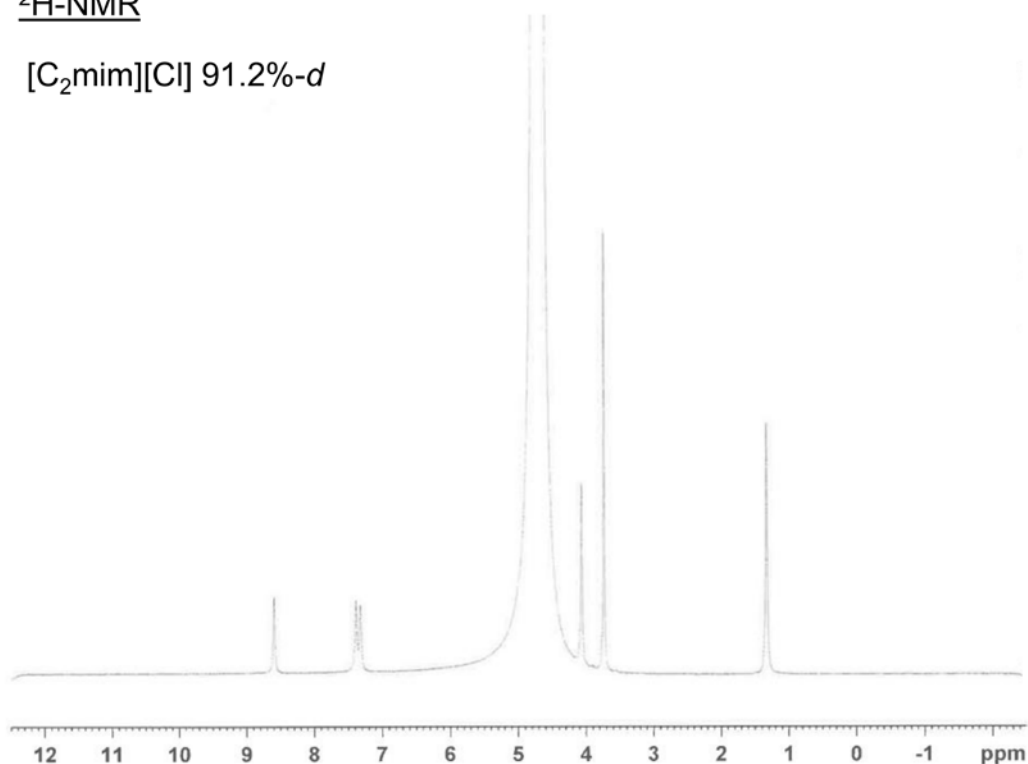


Fig. S3-3. ^2H -NMR (D_2O , 61.4 MHz) of deuterated (91.2%) $[\text{C}_2\text{mim}][\text{Cl}]$.

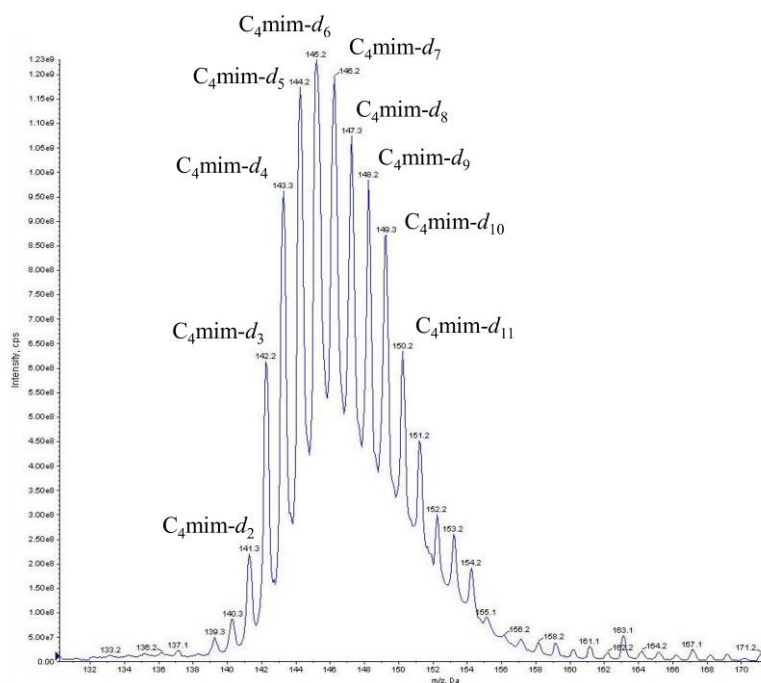


Fig. S4. Electrospray ionization mass spectra in positive mode of C_4mim cation showing the mass distribution of the different isotopologues, which ranges from d_2 – d_{11} . The distribution of the isotopologues is as follows (M^+): 2.4 %, d_2 ; 6.0 %, d_3 ; 9.3 %, d_4 ; 12.0 %, d_5 ; 20.6 %, d_6 ; 14.6 %, d_7 ; 10.9 %, d_8 ; 7.4 %, d_9 ; 8.4 %, d_{10} ; 8.4 %, d_{11} .

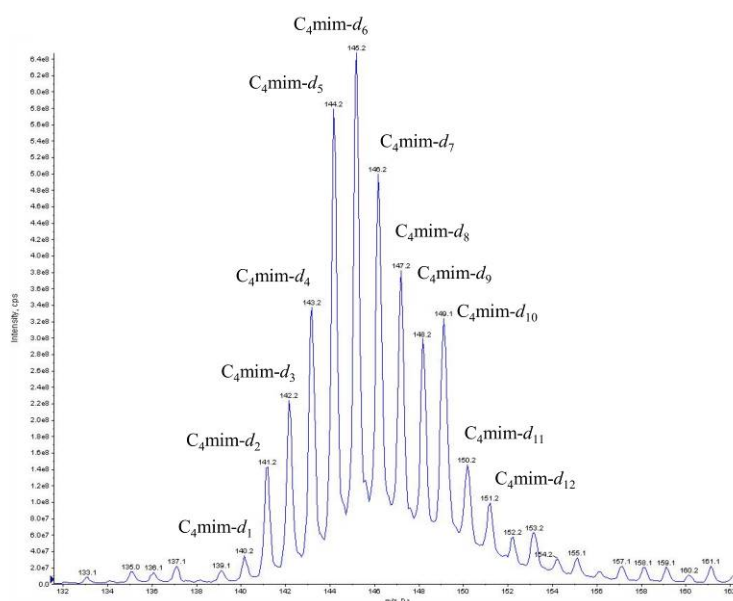


Fig. S5. Electrospray ionization mass spectra in positive mode of C₄mim cation showing the mass distribution of the different isotopologues, which ranges from *d*₁–*d*₁₂. The distribution of the isotopologues is as follows (*M*⁺): 1.1 %, *d*₁; 4.6 %, *d*₂; 6.2 %, *d*₃; 9.8 %, *d*₄; 14.7 %, *d*₅; 15.7 %, *d*₆; 13.1 %, *d*₇; 10.2 %, *d*₈; 8.5 %, *d*₉; 8.2 %, *d*₁₀; 4.7 %, *d*₁₁; 3.3 %, *d*₁₂.

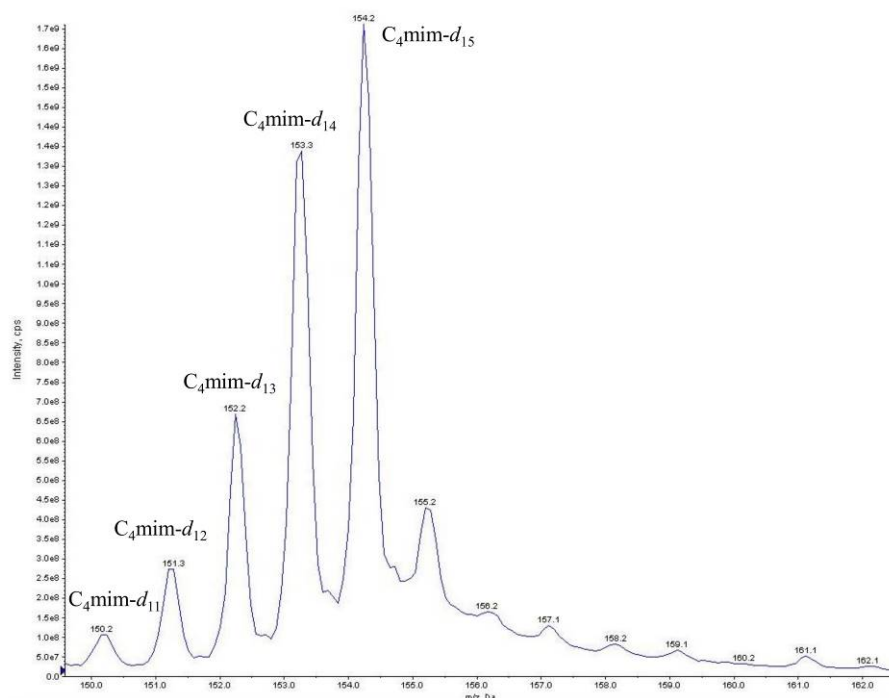


Fig. S6. Electrospray ionization mass spectra in positive mode of C₄mim cation showing the mass distribution of the different isotopologues, which ranges from *d*₁₁–*d*₁₅. The distribution of the isotopologues is as follows (*M*⁺): 3.2 %, *d*₁₁; 7.1 %, *d*₁₂; 15.6 %, *d*₁₃; 32.9 %, *d*₁₄; 41.1 %, *d*₁₅.

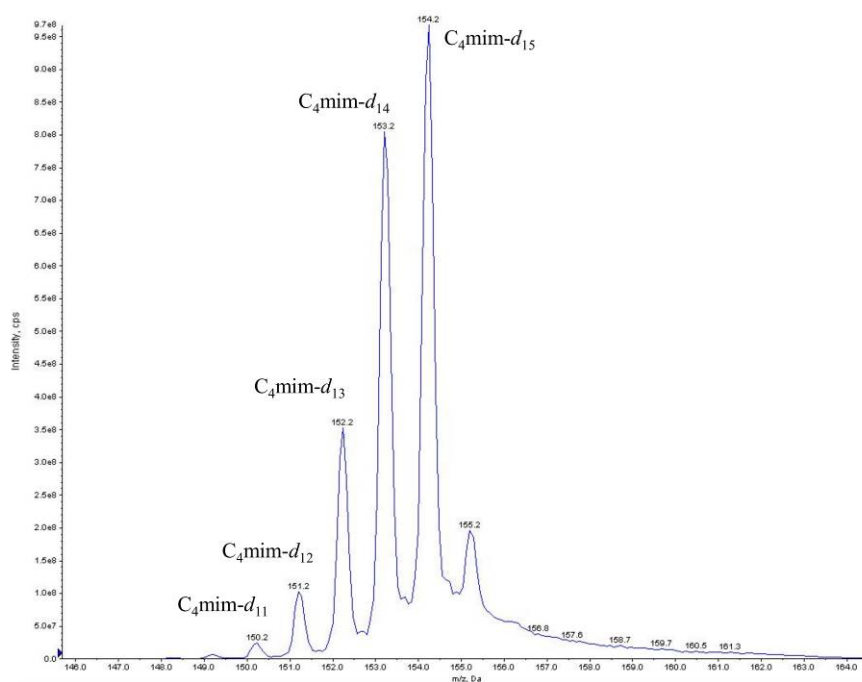


Fig. S7. Electrospray ionization mass spectra in positive mode of C_4mim cation showing the mass distribution of the different isotopologues, which ranges from d_{11} – d_{15} . The distribution of the isotopologues is as follows (M^+): 1.0 %, d_{11} ; 4.4 %, d_{12} ; 14.8 %, d_{13} ; 34.9 %, d_{14} ; 44.8 %, d_{15} .

1H -NMR

$[C_4mim][Cl]$ 94.5%- d

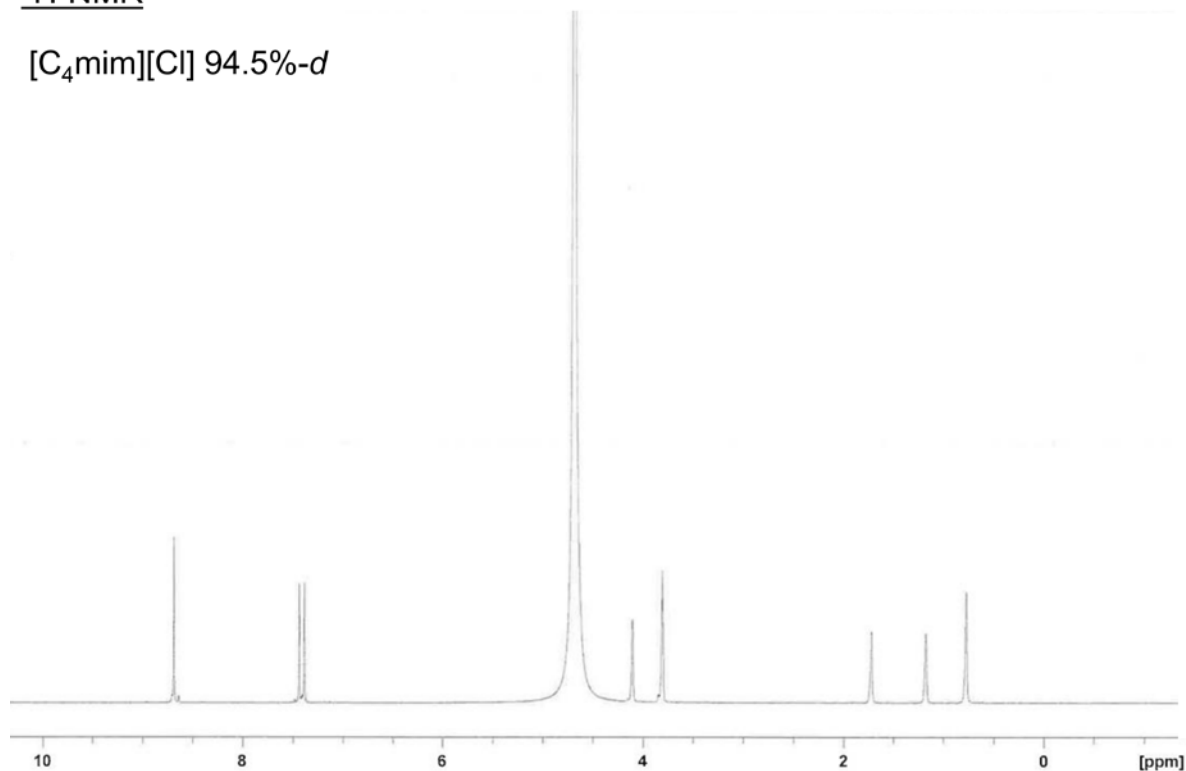


Fig. S7-2. 1H -NMR (D_2O , 400 MHz) of deuterated (94.5%) $[C_4mim][Cl]$.

^2H -NMR

$[\text{C}_4\text{mim}][\text{Cl}]$ 94.5%- d

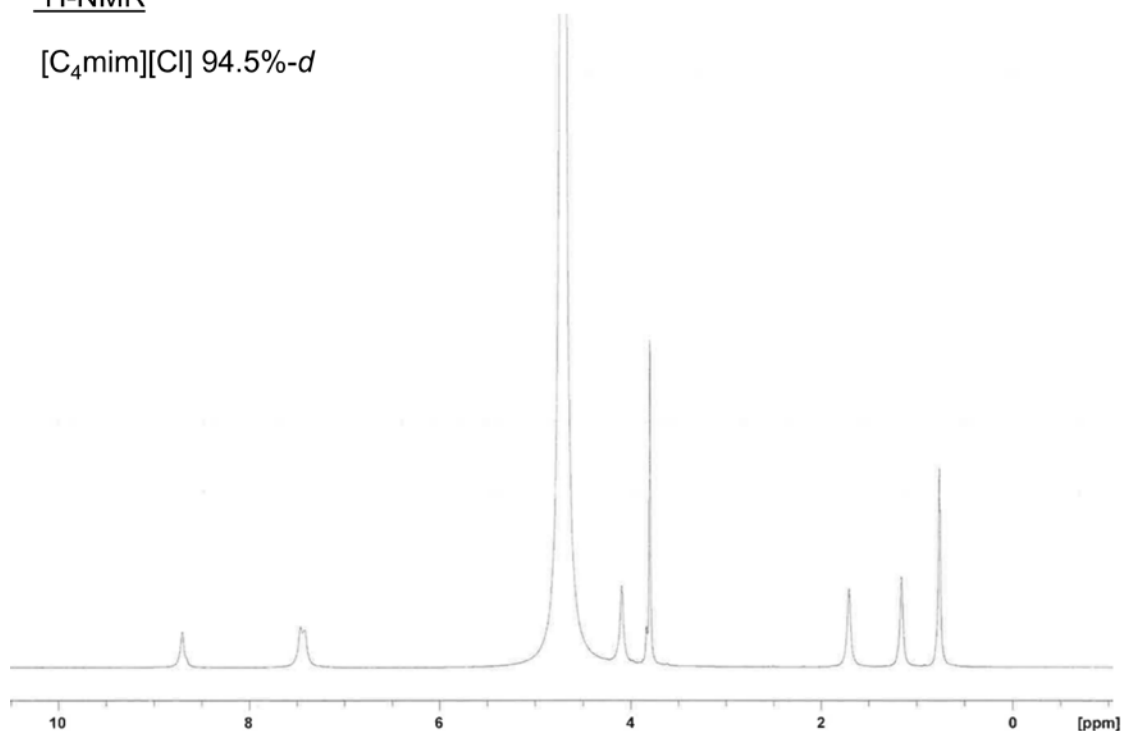


Fig. S7-3. ^2H -NMR (D_2O , 61.4 MHz) of deuterated (94.5%) $[\text{C}_4\text{mim}][\text{Cl}]$.

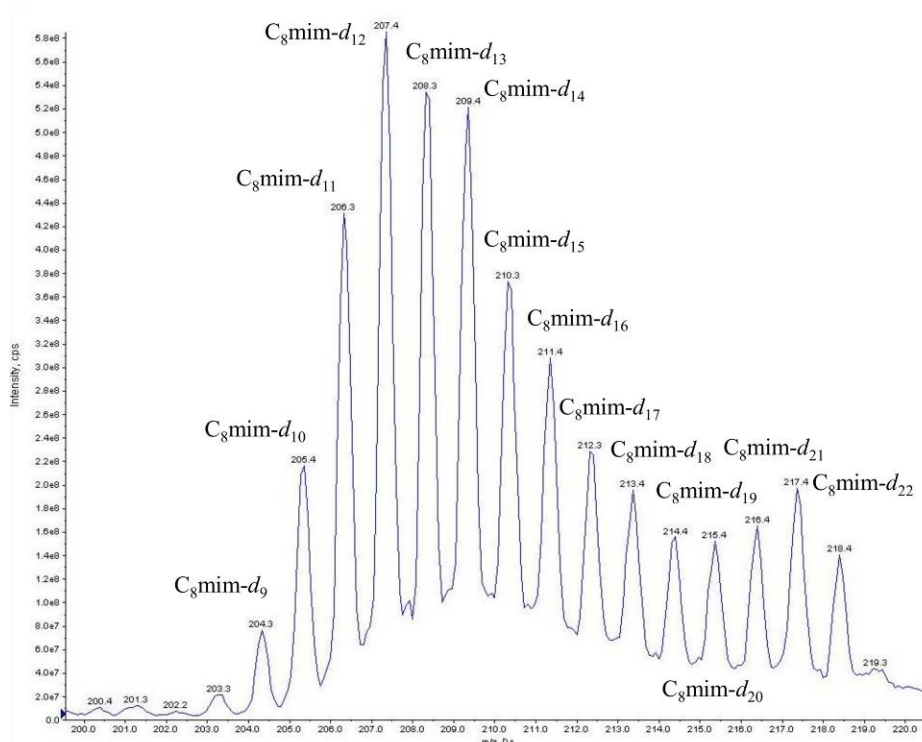


Fig. S8. Electrospray ionization mass spectra in positive mode of C_8mim cation showing the mass distribution of the different isotopologues, which ranges from d_9 – d_{22} . The distribution of the isotopologues is as follows (M^+): 1.8 %, d_9 ; 5.0 %, d_{10} ; 9.6 %, d_{11} ; 13.6 %, d_{12} ; 10.8 %, d_{13} ; 13.7 %, d_{14} ; 8.6 %, d_{15} ; 8.7 %, d_{16} ; 5.4 %, d_{17} ; 5.6 %, d_{18} ; 3.5 %, d_{19} ; 4.2 %, d_{20} ; 4.1 %, d_{21} ; 5.3 %, d_{22} .

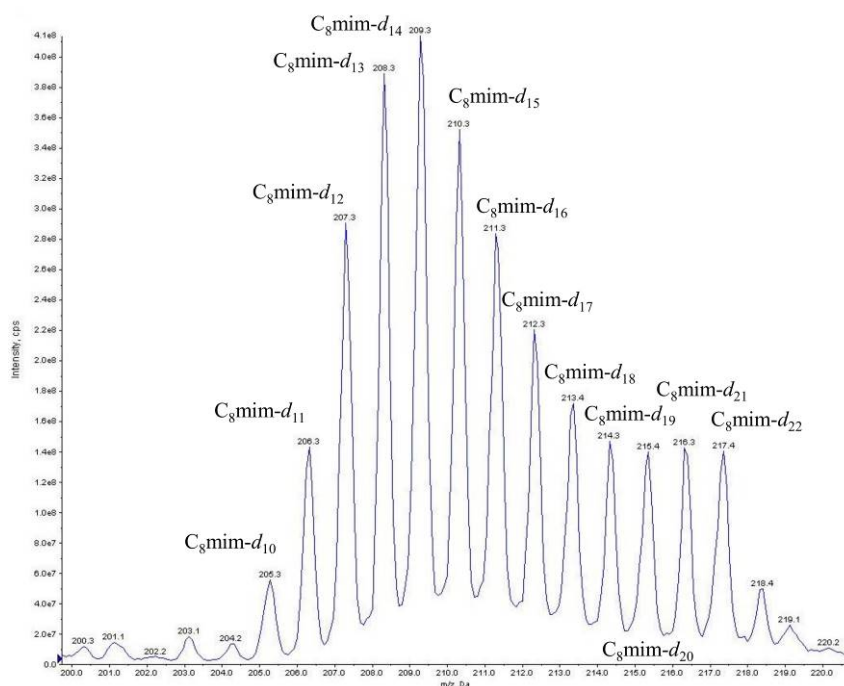


Fig. S9. Electrospray ionization mass spectra in positive mode of C₈mim cation showing the mass distribution of the different isotopologues, which ranges from *d*₁₀–*d*₂₂. The distribution of the isotopologues is as follows (M⁺): 2.2 %, *d*₁₀; 4.7 %, *d*₁₁; 9.8 %, *d*₁₂; 12.2 %, *d*₁₃; 14.7 %, *d*₁₄; 11.6 %, *d*₁₅; 10.8 %, *d*₁₆; 7.4 %, *d*₁₇; 6.3 %, *d*₁₈; 5.1 %, *d*₁₉; 5.1 %, *d*₂₀; 4.6 %, *d*₂₁; 5.4 %, *d*₂₂.

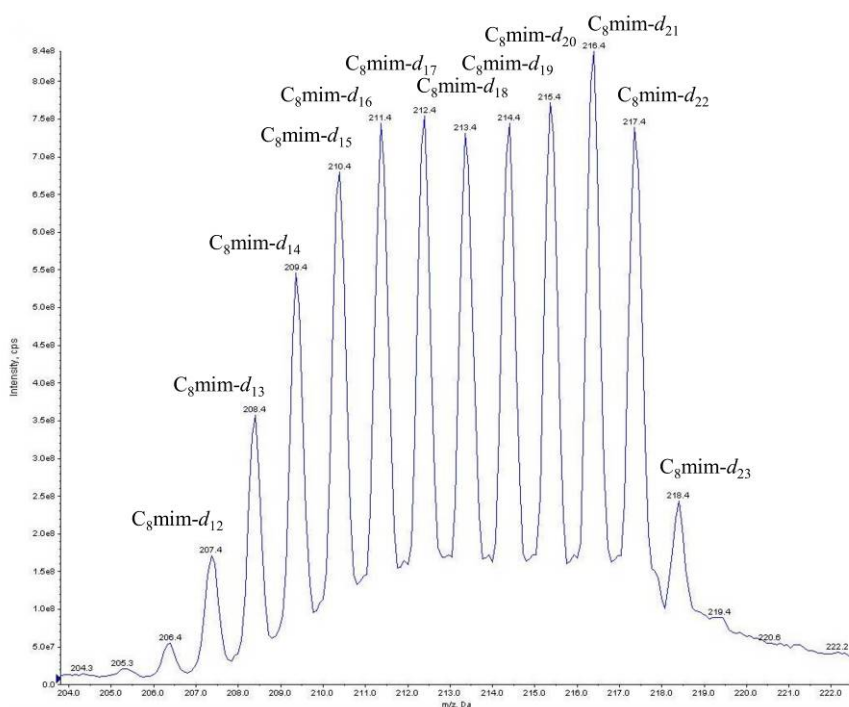


Fig. S10. Electrospray ionization mass spectra in positive mode of C₈mim cation showing the mass distribution of the different isotopologues, which ranges from *d*₁₂–*d*₂₃. The distribution of the isotopologues is as follows (M⁺): 2.6 %, *d*₁₂; 4.8 %, *d*₁₃; 7.5 %, *d*₁₄; 9.8 %, *d*₁₅; 10.2 %, *d*₁₆; 10.6 %, *d*₁₇; 9.1 %, *d*₁₈; 10.1 %, *d*₁₉; 9.7 %, *d*₂₀; 11.3 %, *d*₂₁; 10.6 %, *d*₂₂; 3.6 %, *d*₂₃.

^1H -NMR

$[\text{C}_8\text{mim}][\text{Cl}]$ 78.4%-d

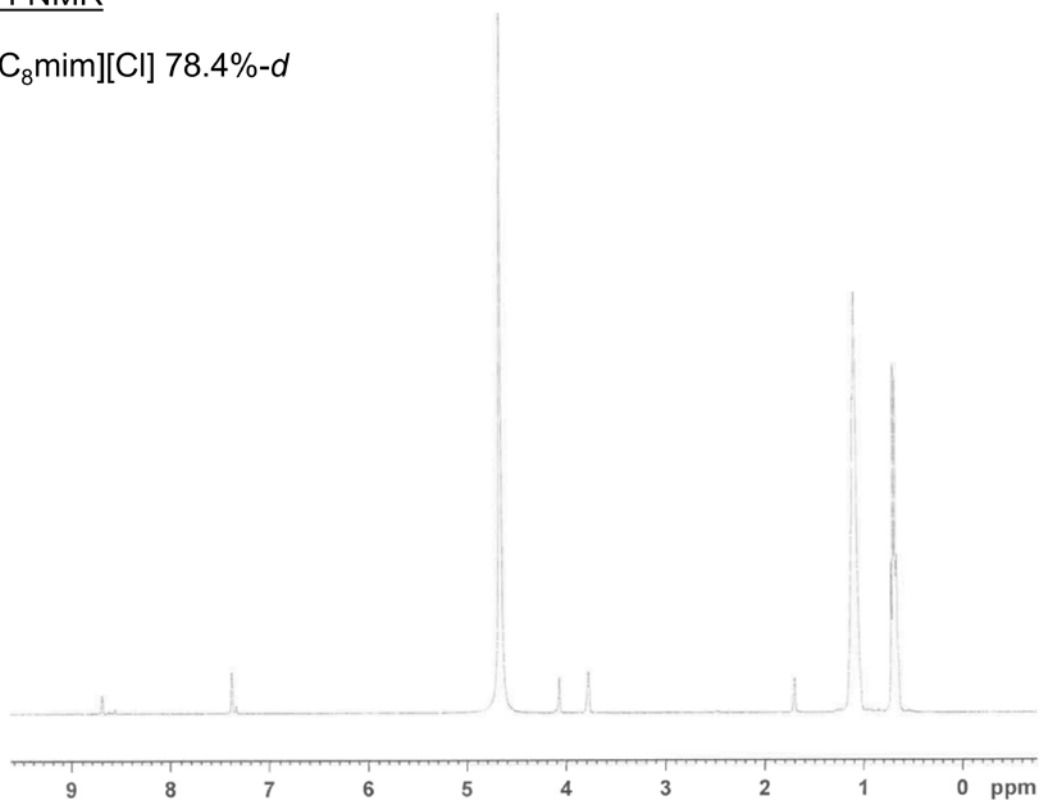


Fig. S10-2. ^1H -NMR (D_2O , 400 MHz) of deuterated (78.4%) $[\text{C}_8\text{mim}][\text{Cl}]$.

^2H -NMR

$[\text{C}_8\text{mim}][\text{Cl}]$ 78.4%-d

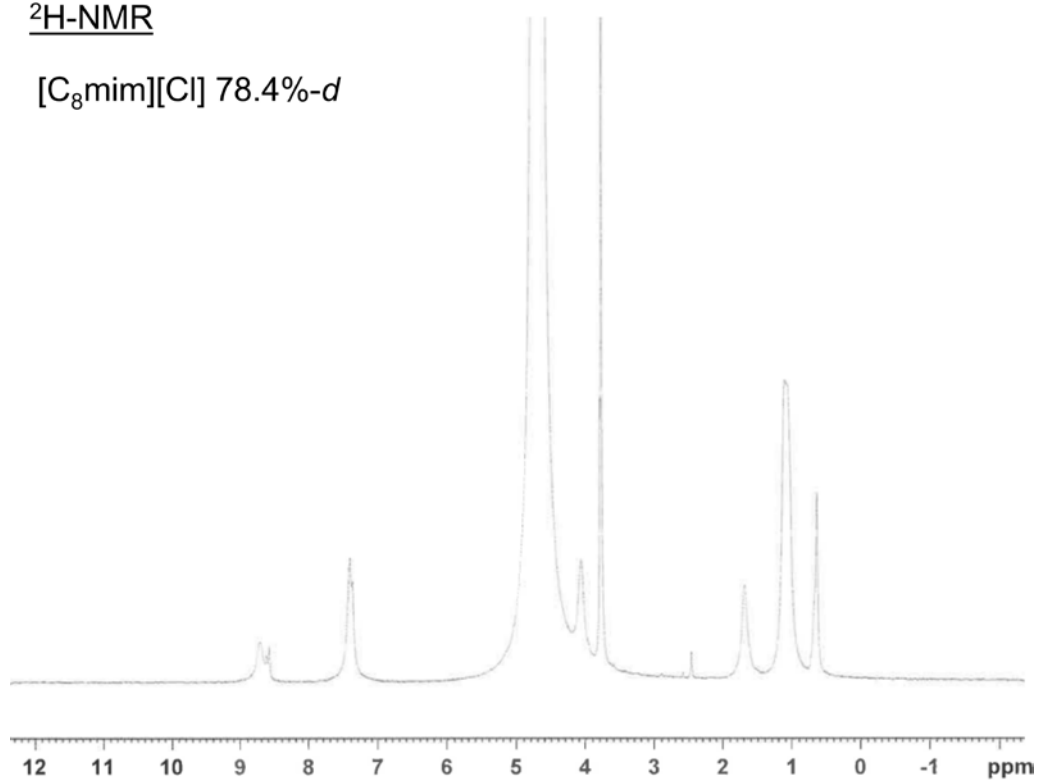


Fig. S10-3. ^2H -NMR (D_2O , 61.4 MHz) of deuterated (78.4%) $[\text{C}_8\text{mim}][\text{Cl}]$.

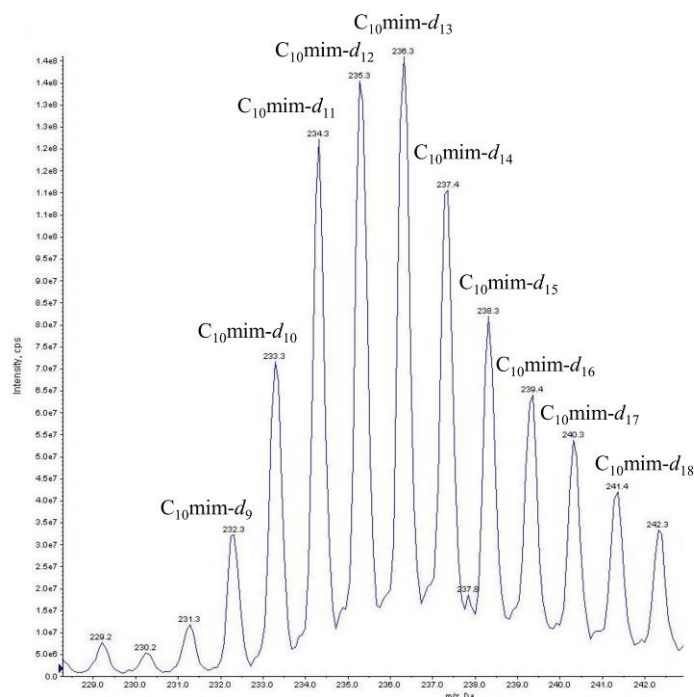


Fig. S11. Electrospray ionization mass spectra in positive mode of C₁₀mim cation showing the mass distribution of the different isotopologues, which ranges from d₉–d₁₈. The distribution of the isotopologues is as follows (M⁺): 4.0 %, d₉; 8.3 %, d₁₀; 13.7 %, d₁₁; 15.2 %, d₁₂; 16.6 %, d₁₃; 13.9 %, d₁₄; 8.7 %, d₁₅; 8.7 %, d₁₆; 5.8 %, d₁₇; 5.1 %, d₁₈.

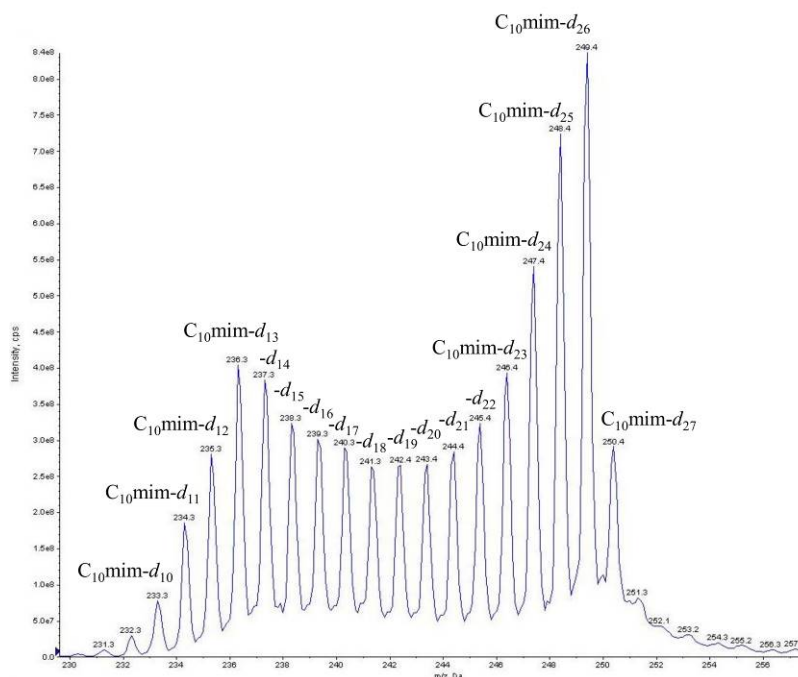


Fig. S12. Electrospray ionization mass spectra in positive mode of C₁₀mim cation showing the mass distribution of the different isotopologues, which ranges from d₁₀–d₂₇. The distribution of the isotopologues is as follows (M⁺): 1.2 %, d₁₀; 2.6 %, d₁₁; 4.1 %, d₁₂; 5.8 %, d₁₃; 6.3 %, d₁₄; 4.7 %, d₁₅; 5.3 %, d₁₆; 5.0 %, d₁₇; 4.7 %, d₁₈; 4.1 %, d₁₉; 4.5 %, d₂₀; 4.3 %, d₂₁; 5.2 %, d₂₂; 6.2 %, d₂₃;

8.2 %, d_{24} ; 10.1 %, d_{25} ; 12.3 %, d_{26} ; 5.4 %, d_{27} .

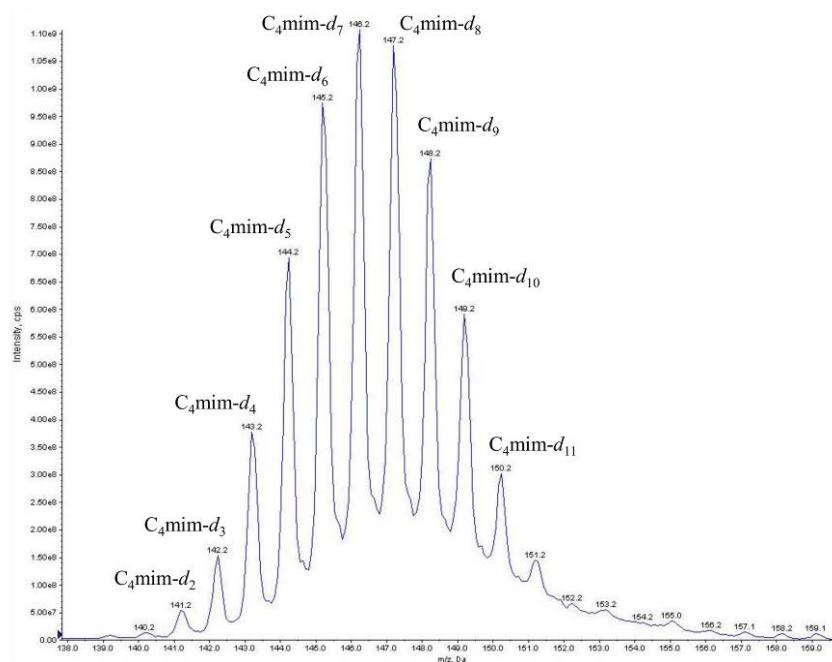


Fig. S13. Electrospray ionization mass spectra in positive mode of C₄mim cation showing the mass distribution of the different isotopologues, which ranges from d_2 – d_{11} . The distribution of the isotopologues is as follows (M^+): 1.0 %, d_2 ; 2.0 %, d_3 ; 5.7 %, d_4 ; 9.4 %, d_5 ; 15.6 %, d_6 ; 18.6 %, d_7 ; 17.3 %, d_8 ; 14.8 %, d_9 ; 10.2 %, d_{10} ; 5.3 %, d_{11} .

¹H-NMR

[C₄mim][Cl] 48.8%-*d*

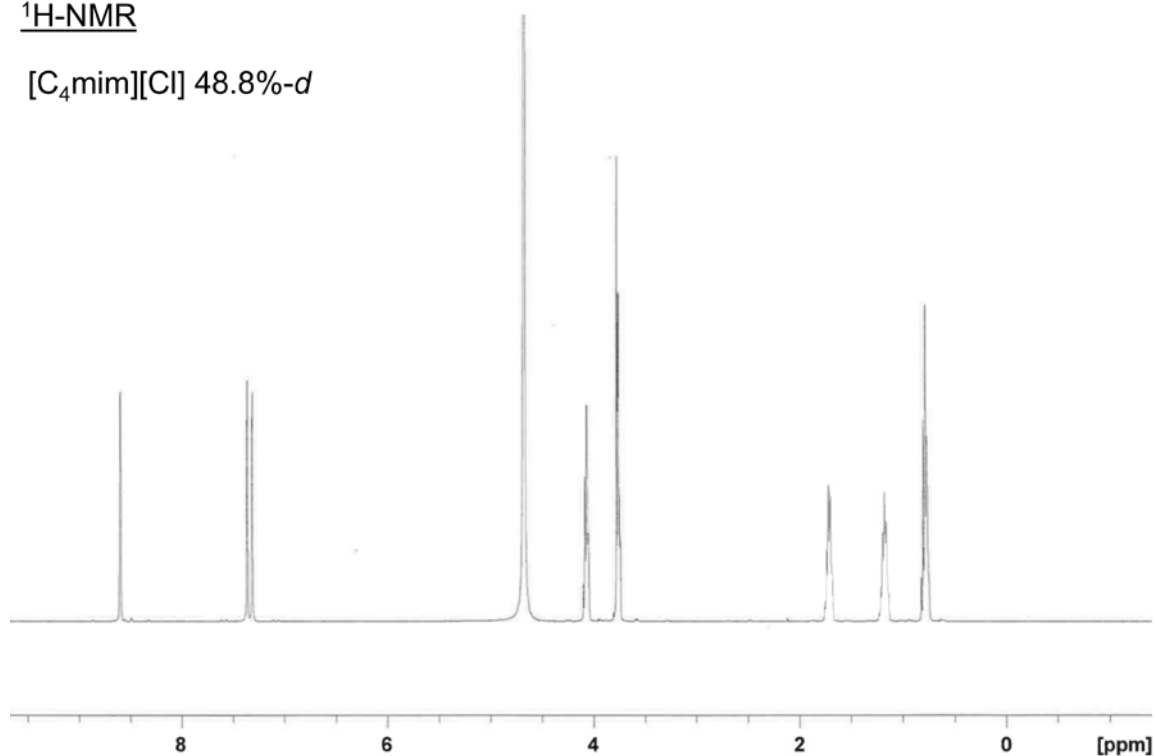


Fig. S13-2. ^1H -NMR (D_2O , 400 MHz) of deuterated (48.8%) $[\text{C}_4\text{mim}][\text{Cl}]$.

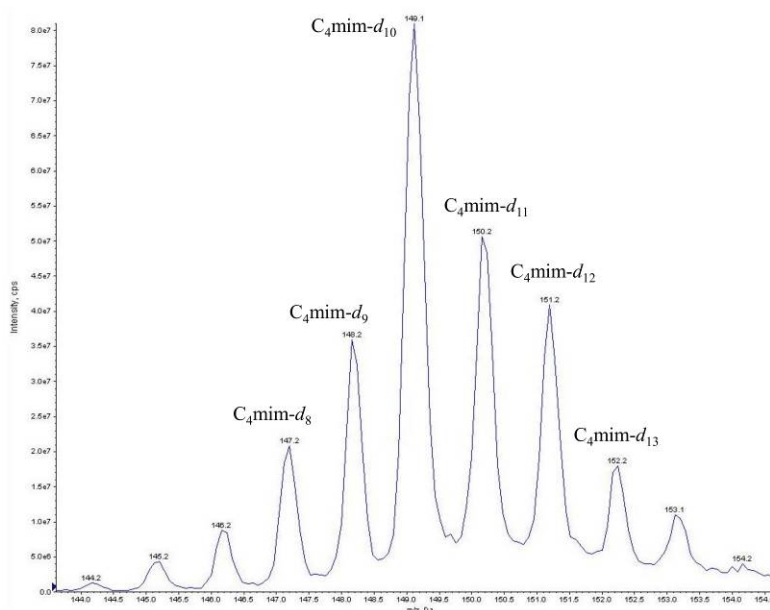


Fig. S14. Electrospray ionization mass spectra in positive mode of C_4mim cation showing the mass distribution of the different isotopologues, which ranges from d_8 – d_{13} . The distribution of the isotopologues is as follows (M^+): 7.9 %, d_8 ; 12.7 %, d_9 ; 34.7 %, d_{10} ; 20.5 %, d_{11} ; 16.7 %, d_{12} ; 7.5 %, d_{13} .

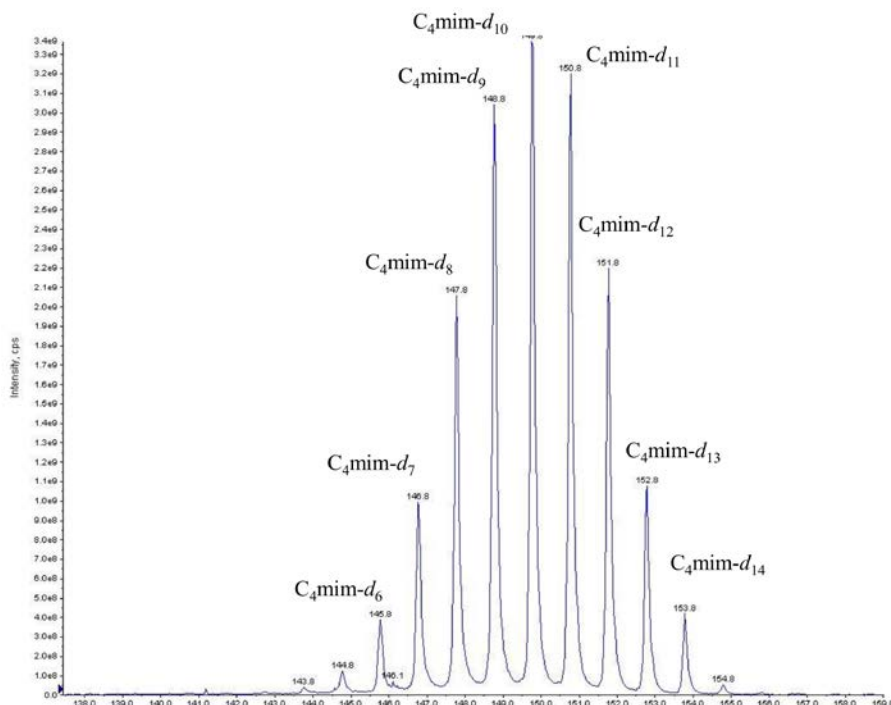


Fig. S15-1. Electrospray ionization mass spectra in positive mode of C_4mim cation showing the mass distribution of the different isotopologues, which ranges from d_6 – d_{14} . The distribution of the isotopologues is as follows (M^+): 2.3 %, d_6 ; 6.4 %, d_7 ; 12.8 %, d_8 ; 18.6 %, d_9 ; 20.6 %, d_{10} ; 18.1 %, d_{11} ; 10.0 %, d_{12} ; 4.0 %, d_{13} ; 1.0 %, d_{14} .

d_{11} ; 12.6 %, d_{12} ; 6.3 %, d_{13} ; 2.3 %, d_{14} .

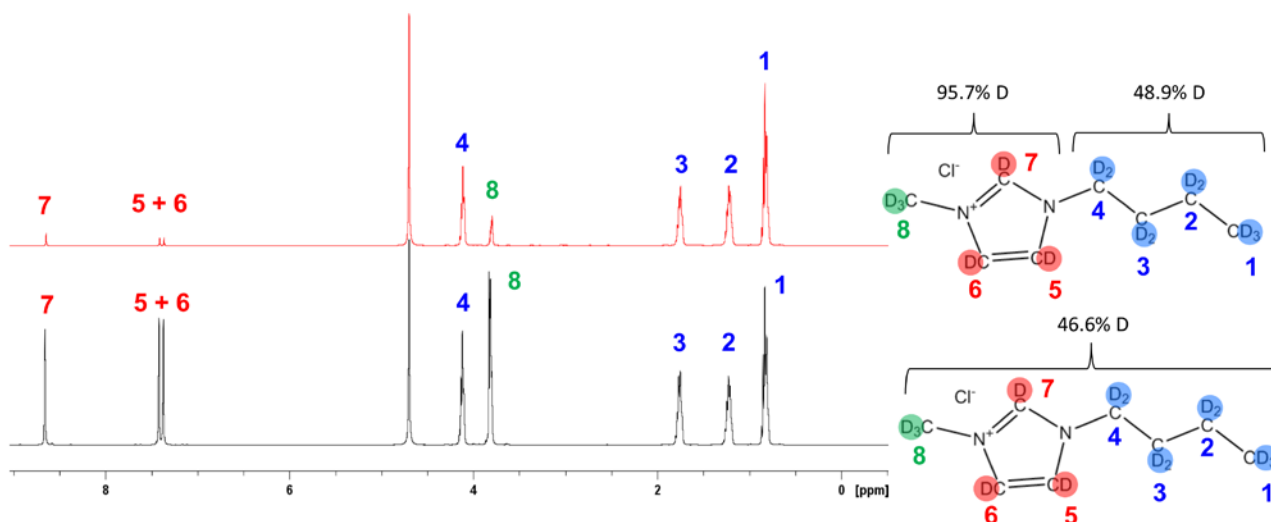


Fig. S15-2. ^1H -NMR (D_2O , 400 MHz) of deuteration level controlled (46.6%) [C₄mim][Cl] and position-selective deuterated (head = 95.7 %, tail = 48.9 %) [C₄mim][Cl].

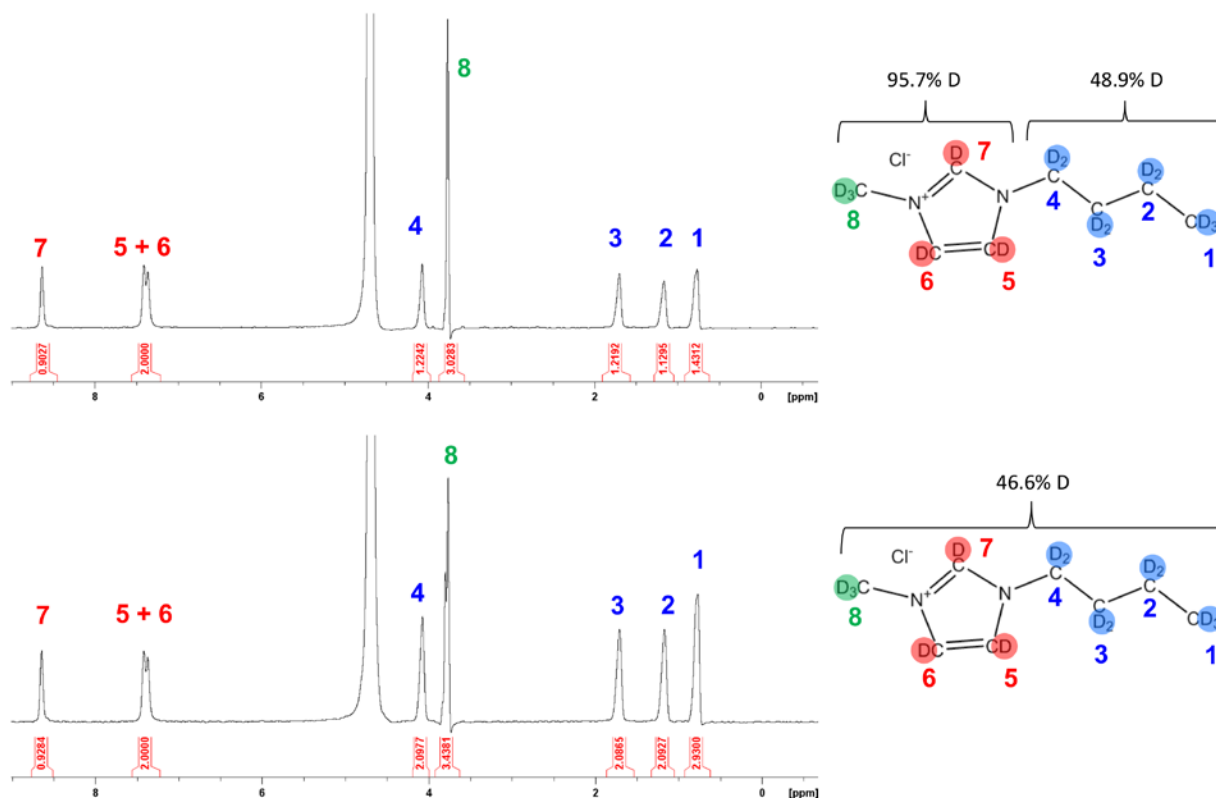


Fig. S15-3. ^2H -NMR (D_2O , 61.4 MHz) of deuteration level controlled (46.6%) [C₄mim][Cl] and position-selective deuterated (head = 95.7 %, tail = 48.9 %) [C₄mim][Cl].

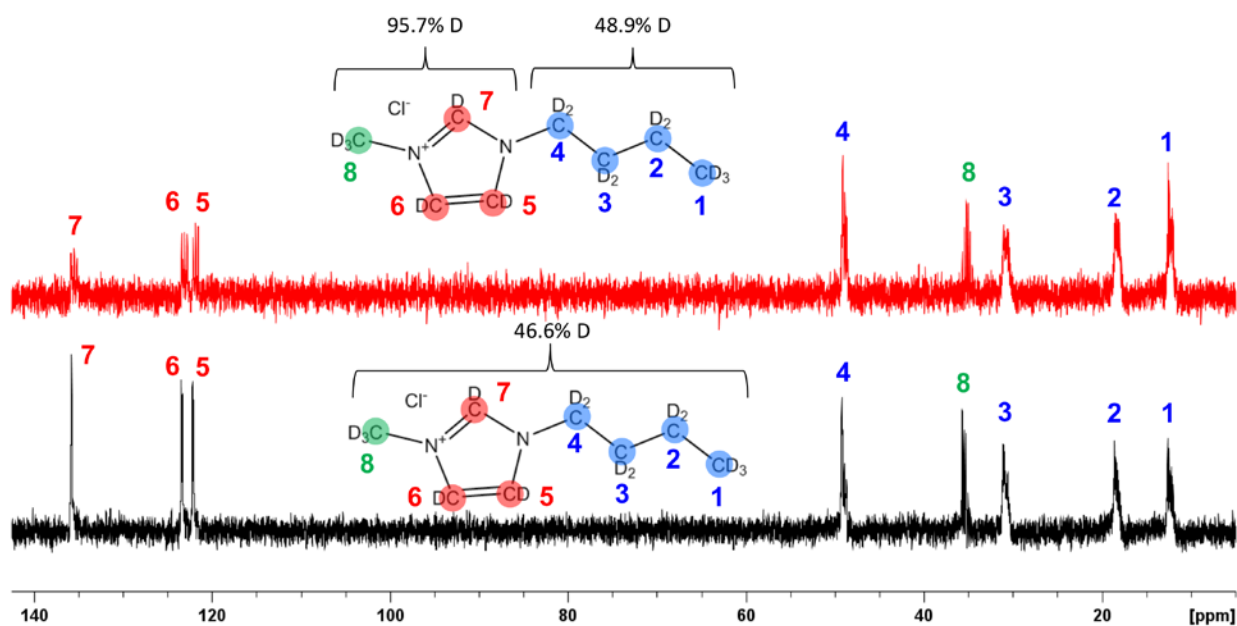


Fig. S15-4. ^{13}C -NMR (D_2O , 400 MHz) of deuteration level controlled (46.6%) [C4mim][Cl] and position-selective deuterated (head = 95.7 %, tail = 48.9 %) [C4mim][Cl].

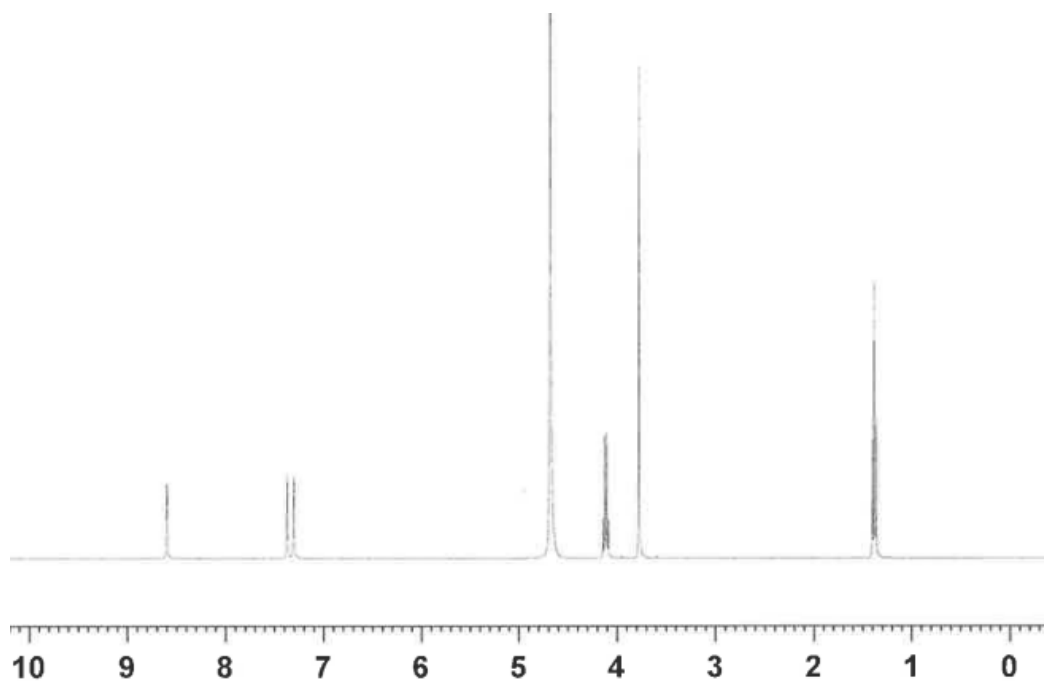


Fig. S16-1. ^1H -NMR (D_2O , 400 MHz) of [C2mim][Cl] (starting material).

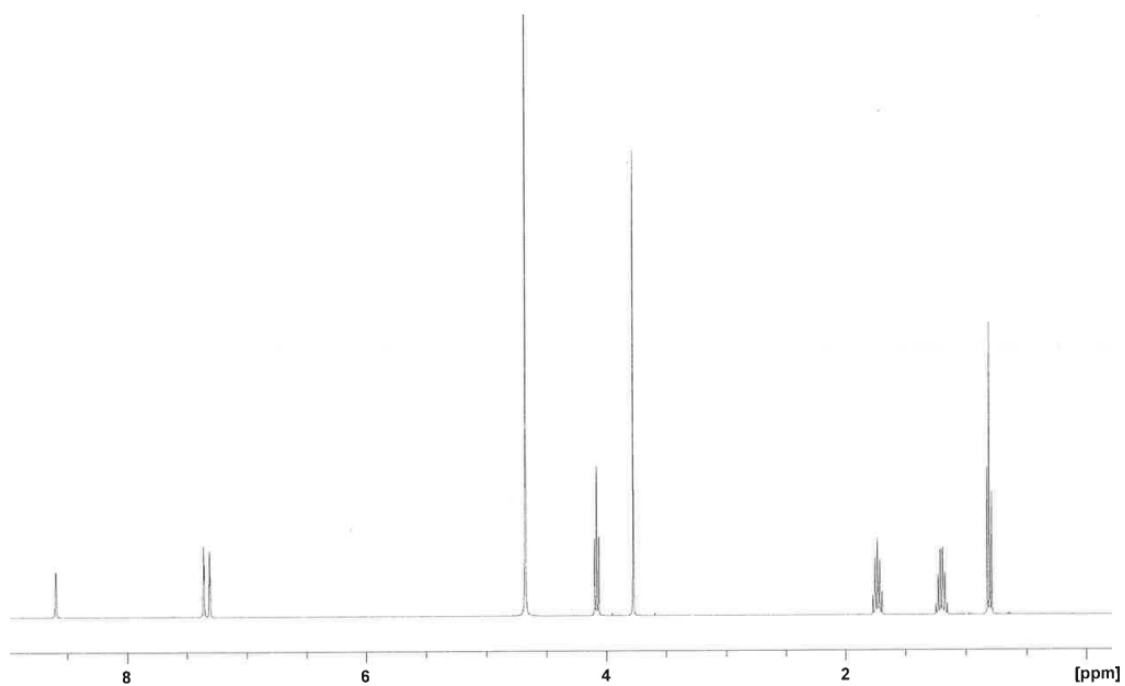


Fig. S16-2. ^1H -NMR (D_2O , 400 MHz) of $[\text{C}_4\text{mim}][\text{Cl}]$ (starting material).

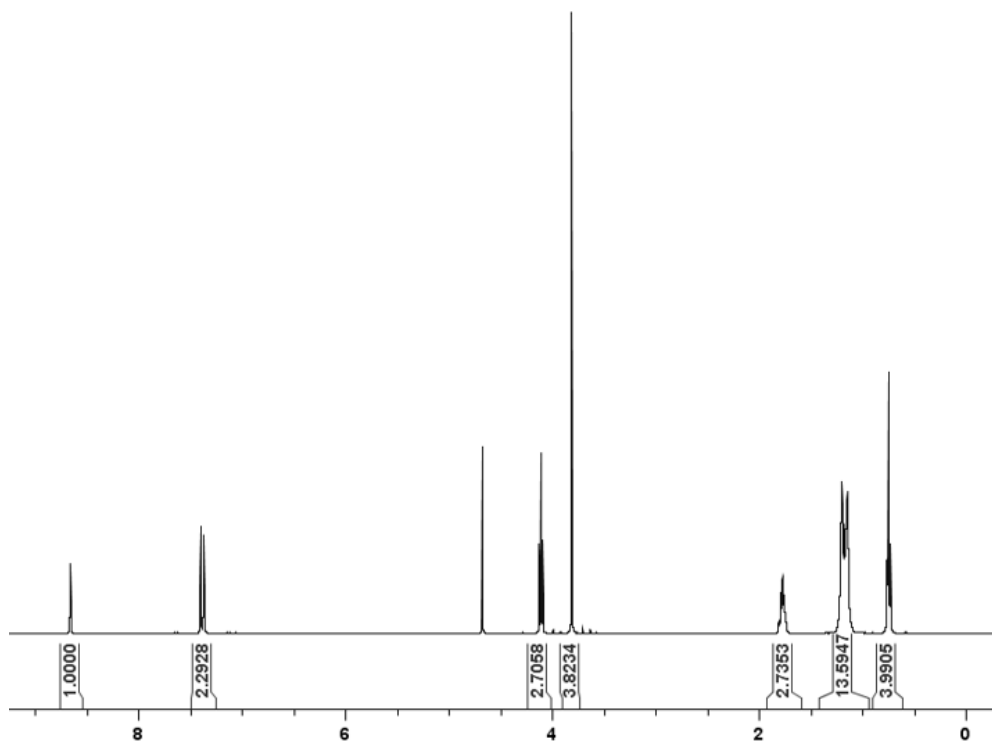


Fig. S16-3. ^1H -NMR (D_2O , 400 MHz) of $[\text{C}_8\text{mim}][\text{Cl}]$ (starting material).

Neutron reflectivity analysis for the position-selective deuterated IL

To estimate the SLD value of the position-selective deuterated [C₄mim][TFSA], the NR measurements of the partially deuterated [C₄mim][TFSA]/SiO₂-wafer sample was performed on a BL17 SHARAKU reflectometer. The critical wave vector for the total external reflection (Q_c), which is defined as $Q_c = 4(\pi\rho)^{1/2}$ (ρ represents the difference of the SLD value between the partially deuterated [C₄mim][TFSA] and SiO₂-wafer sample), was observed around $Q_c = 0.0066$ (\AA^{-1}). Using the obtained Q_c value, the SLD value of the partially deuterated [C₄mim][TFSA] can be estimated to be $4.34 (\times 10^{-6} \text{\AA}^{-2})$.

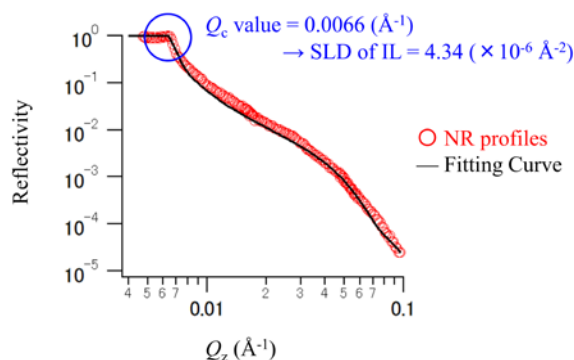


Fig. S16. Neutron reflectivity profiles of the partially deuterated [C₄mim][TFSA]/SiO₂ sample.

References

- 1 T. A. Darwish, E. Luks, G. Moraes, N. R. Yepuri, P. J. Holden and M. James, *J. Label. Compd. Radiopharm.*, 2013, **56**, 520–529.
- 2 Z. K. Reeder, A. M. Adler and K. M. Miller, *Tetrahedron Lett.*, 2016, **57**, 206–209.
- 3 L. S. Bartell, K. Kuchitsu and R. J. DeNeui, *J. Chem. Phys.*, 1961, **35**, 1211–1218.
- 4 N. D. Rebuck, A. A. Conte and L. Stallings, *ASLE Trans.*, 1977, **20**, 108–114.
- 5 K. Akutsu, T. Niizeki, S. Nagayama, N. Miyata, M. Sahara, A. Shimomura, M. Yoshii and Y. Hasegawa, *J. Ceram. Soc. Japan*, 2016, **124**, 172–176.
- 6 A. Nelson, *J. Appl. Crystallogr.*, 2006, **39**, 273–276.